THEORETICAL ACOUSTIC BENEFIT OF HIGH BYPASS RATIO AND VARIABLE-AREA NOZZLE IN TURBOFAN ENGINES

A. Moreau

DLR, Institute of Propulsion Technology
Dpt. of Engine Acoustics, Berlin, Germany
antoine.moreau@dlr.de

ABSTRACT

This paper documents the acoustic benefit that can be expected from a variable-area nozzle (VAN) implemented in turbofan engines with different design fan pressure ratio. To address this question, a fast meanline approach provides an aerodynamic design and the location of the acoustic certification points within the fan map; then, the overall sound power levels from the jet and from the fan stage are calculated based on well-established empirical correlations and an analytical method. Both models predict an increasing overall acoustic benefit of the VAN as the engine bypass ratio gets larger, which is essentially related to the aerodynamic unloading of the fan stage as the nozzle is opened. The jet noise reduction is confirmed, and it is found out that fan tonal noise may slightly increase while fan broadband noise may be substantially reduced. This is of particular interest, since fan broadband noise dominates in ultra high-bypass-ratio engines.

KEYWORDS

VARIABLE-AREA NOZZLE, TURBOFAN ENGINE, FAN NOISE PREDICTION, ANALYTICAL METHOD

NOMENCLATURE

DP/SL/CB/AP operating points: cruise/take-off sideline/take-off cutback/landing approach
FPR stagnation-pressure ratio of the fan stage
M_j, M_{tr} jet exhaust and rotor relative tip Mach numbers
OAPWL overall sound powel level rel. to 10^{-12} W
VAN variable-area nozzle
ω aerodynamic loss coefficient of the rotor at the meanline radius

INTRODUCTION

Over the past decades the size of civil-aircraft turbofan aero-engines has steadily increased to meet aerodynamic-efficiency and noise-levels requirements. Indeed, larger engines may be designed for the same thrust with a lower fan pressure ratio (FPR) and a lower exhaust jet velocity, which are two key parameters for achieving high propulsive efficiency and low acoustic emission. Theoretical studies by NASA (Guynn et al., 2000) or DLR (Moreau, 2017) have demonstrated and provided a rationale for the benefit of such engines, mostly attributable to the reduction of the flow Mach numbers both within the fan stage and in the jet. Currently, the trend towards engines with an ultra-high bypass ratio (UHBR) beyond 12 (accordingly, FPR < 1.4) is actively followed by research and industry, as for example the EU-funded ENOVAL project shows (Merkl, 2018).

However, as the design fan pressure ratio is reduced below 1.4, the implementation of a variable-geometry system is needed for the fan to operate in a stable aerodynamic and aeroelastic domain at off-design points, especially take-off and approach. As explained by Cumpsty (2009), this is because the nozzle unchokes ($M_j < 1$) at low flight Mach number with these low-FPR designs, which limits the mass flow capacity of the fan and shifts the take-off and approach operating points closer to the fan surge line. One of the technical solutions is the variable-area nozzle (VAN), which can be opened at take-off and approach conditions, thereby unloading the fan blades and ensuring stable operation.

Several engine-cycle studies from Cranfield University (Kyritsis, 2006; Giannakakis, 2013) quantified the thermodynamic benefit of the VAN. The mechanical feasibility study by Sain et al. (2015) within the ENOVAL project indicates that the VAN is seriously considered to be implemented in future aero-engines. More recently, the work by Kavvalos et al. (2019) showed based on modern aerodynamic design tools that a substantial gain in surge margin by up to 25% can be achieved at take-off with a VAN opening by 20% from its nominal area, on a boundary-layer-ingesting aft-fan with FPR=1.2 at design.

To the author's knowledge, only few studies have been dedicated so far to the acoustic impact of the VAN, and none has provided a quantitative prediction of its impact on fan noise specifically. Michel (2011) estimated from an analytical jet noise model that around 2 dB reduction in jet mixing noise can be expected for take-off and approach, with an area opening by 15%. Woodward et al. (2004, 2006) determined experimentally on the NASA SDT fan stage that an overall noise reduction by 2 dB can be obtained, whereby fan broadband noise is significantly reduced and fan tones are slightly amplified. The purpose of the present paper is to provide a more systematic assessment of the acoustic benefit of the VAN implemented on various engine designs (with fan pressure ratios FPR between 1.3 and 1.6) which all produce the same thrust and are thus comparable. For the first time, the VAN impact on the tonal and broadband components of fan noise is evaluated theoretically.

METHODOLOGY AND FAN CONFIGURATIONS

This section explains the procedure adopted to assess the acoustic impact of a VAN for engines with different values of design fan pressure ratio. It also details the geometry and aerodynamic characteristics of each engine configuration.

Methodology

A multi-disciplinary thermodynamic/aerodynamic/acoustic approach is applied according to Moreau (2017), and summarized in Fig.1. It is based on the aerodynamic performance evaluation of the fan stage and the calculation of its related flow parameters along a single representative streamline through the fan, called the meanline. For each engine specification, a fan geometry is designed to provide optimal performance at mid-cruise (DP), then the full aerodynamic fan map is calculated and the position of the off-design acoustic certification points is determined within that map. For the case with VAN, the optimal nozzle area opening is determined by maximizing the fan isentropic efficiency at each off-design point. We will see later that this procedure also automatically improves the surge margin, which is the primary motivation for implementing a VAN. Finally, the noise levels are calculated at the off-design points with different acoustic models. In all calculations, no acoustic treatment is implemented in the intake and exhaust duct sections. Jet noise is estimated with the model developped by Stone (1983). For the fan noise component, two different models are used. An analytical method (details in Moreau, 2017) models each sound generation mechanism separately. In this method we have the tonal and broadband components of the rotor-wake - stator interaction, where the overall

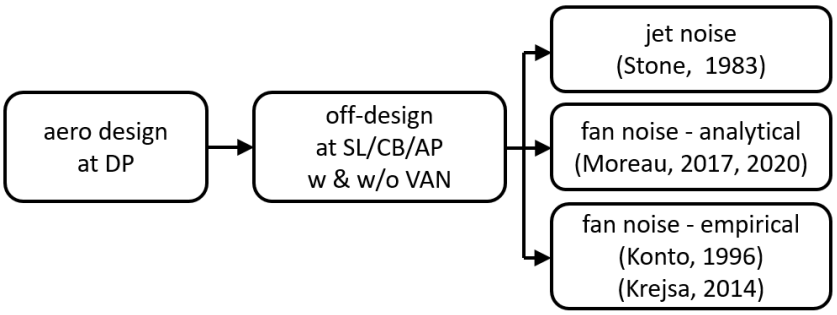

Figure 1: **Engine noise evaluation procedure**

sound power scales roughly as follows:

$$\text{OAPWL} = 10\log_{10}\left(V \cdot (kc)^2 \cdot \mathcal{L}^2 \cdot M^4 \cdot \omega^2\right) + \text{const.}, \tag{1}$$

here, the scaling parameters are the stator vane count V, reduced wavenumber kc, aero-acoustic transfer function $\mathcal{L}$, and most importantly the flow Mach number M and the rotor loss coefficient ω which is a measure of the rotor wake size responsible for the sound generation on the stator vanes. The analytical method also considers the tonal rotor self-noise component, called buzz-saw noise and dominating the sound field of supersonic fan stages, this non-linear source is also calculated analytically according to Moreau (2020). Alternatively, we apply empirical correlations obtained by NASA from static engine tests as documented by Kontos (1996) and Krejsa (2014). In this model illustrated in Eq.(2), the overall sound power scales with global stage parameters such as the mass flow Q and the stagnation enthalpy rise ΔT_t.

$$\text{OAPWL} = 10\log_{10}\left(Q \cdot \Delta T_t^n\right) + \text{const., with } \left[\begin{array}{l} n = 2, \text{ Kontos (1996)} \\ n = 4, \text{ Krejsa (2014)} \end{array}\right. \tag{2}$$

Aircraft application and fan designs

Four different engines with their design fan pressure ratio varying from 1.3 to 1.6 are considered in this study. For the sake of a proper and fair acoustic evaluation, all engines are sized for the same aircraft application which is a single-aisle mid-range civil aircraft powered by two turbofan engines, with a maximum take-off and maximum landing weight of 78 and 66 tons respectively. The flight conditions and thrust requirements at the design point and off-design acoustic certification points are detailed in the following Table 1. As all engines operate with the same thrust at all points considered, their acoustic emissions can be compared.

Table 1: **Flight conditions for each operating point**

	design/mid-cruise	take-off sideline	take-off cutback	landing approach
	DP	SL	CB	AP
flight Mach nb.	0.78	0.21	0.35	0.21
flight altitude	10500m	0	500m	120m
req. total thrust	35kN	167kN	110kN	53kN

For each of the engines considered, a set of parameters has been specified to allow for comparable fan designs. In the following Table 2, the left part a) details the parameters common to all designs. The total engine length and the length of the intake have been maintained constant

to avoid a too heavy engine when the fan diameter increases. We will see later that this constraint partly limits the acoustic benefit of large engines. Traditional design values are taken for the rotor-face axial number M_x, the work coefficient ψ, and the diffusion factor DF of the rotor and stator blades at meanline. Also the blade aspect ratio AR and the profile relative thickness t/c assume values typical of aero-engine fan stages. In the right part b) of the table, the parameters specific to each of the four designs are detailed. With increasing design fan pressure ratio FPR and constant ψ, the design tip relative Mach number increases; the rotor must be equipped with more blades B to sustain the increased pressure gradient. The number of stator vanes V is chosen mostly for acoustic reasons: here we take V=2B+4 in order to ensure a cut-off design of the first blade-passing frequency tone at all conditions. Finally, the fan diameter decreases with increasing FPR. Values for the engine bypass ratio BPR are provided as indications for the range of engines considered, but the true independent variable and actually physically relevant driver both for fan-stage aerodynamics and acoustics is the fan pressure ratio FPR, as Cumpsty (2009) pointed out. The variations of the blade passing frequency, which is the product of rotor blade count by rotation frequency, are also provided: it will be discussed later on how the shift towards low frequencies observed when decreasing the fan pressure ratio may affect the fan noise levels.

Table 2: **Fan design parameters**

a)

L_{tot}/L_{in}	2.7m/0.9m	rotor AR	2
M_x	0.6	rotor t/c	0.02
ψ	0.3	stator AR	4
DF	0.45	stator t/c	0.06

b)

FPR	1.3	1.4	1.5	1.6
BPR	15.5	11.6	9.3	7.7
D in m	2.10	1.88	1.72	1.60
M_{tr}	1.04	1.14	1.23	1.32
B/V	16/36	18/40	22/48	26/56
N in rpm	2546	3231	3948	4617
f_{BPF} in kHz	0.7	1	1.5	2

A simplified view of the different fan geometries is given in Fig.2. The fan diameter gets larger as the design fan pressure ratio decreases, while the total engine length is kept constant; note that the distance between rotor and stator is therefore reduced relative to the dimensions of the fan blades. All calculations have been carried out in hardwall conditions, but it should highlighted that liners may have a different acoustic impact depending on the fan design, especially when the ratio of intake liner length to fan diameter is reduced along the design FPR change. Also, the core engine is not considered and a single stream is modelled with the overall mass flow through the bypass and core stream of the actual engine. Therefore, the values for the engine bypass ratio BPR given in Table 2 are estimated from a virtual constant datum core whose size and thermodynamic parameters (e.g. overall pressure ratio OPR=40 and turbine entry temperature TET=1545K) are common to all designs according to the correlation proposed by Moreau (2017). The blade profiles are shown in the right part of Fig.2, in a cut view taken at the meanline radius. Two profiles are shown exemplarily for each blade row and configuration. With decreasing FPR, the blade solidities are reduced by an amount roughly proportional to the blade count variations, and the mean stagger angles are slightly reduced, too.

Impact of the VAN on the operating points

As explained before, for each of the fan configurations, the associated aerodynamic performance map has been calculated by varying constinuously the mass flow and increasing the rotation speed from 50% to 110% of the design speed. The four maps are presented in Fig.3

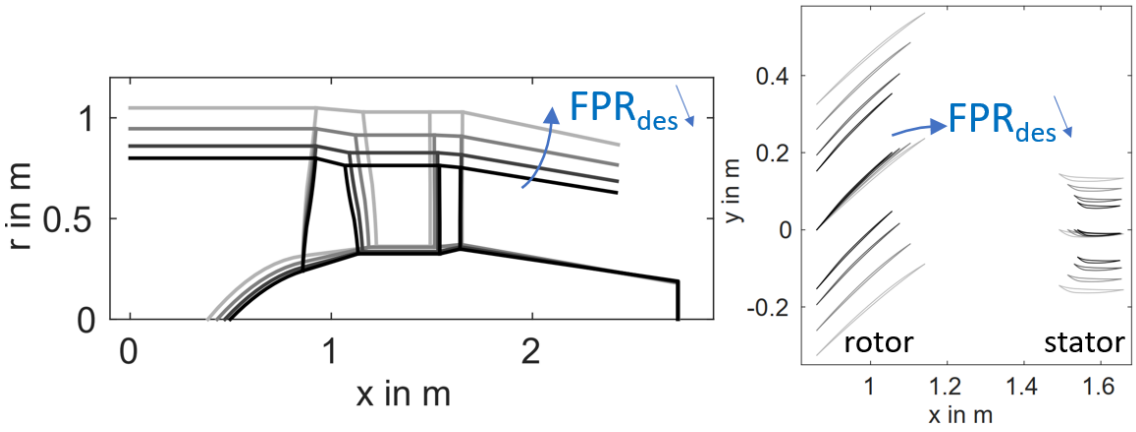

Figure 2: **Overview of the fan stage geometry: side view in the meridional S2 plane (left) and blade profiles at meanline radius in the blade-to-blade S1 plane (right)**

with solid lines depicting the constant-speed lines of the fan map, coloured from dark grey for a design FPR of 1.6 to light grey for FPR=1.3. The vertical axis, corresponding to the current value of FPR in the map, is normalized such that all four fans have their respective design point located at the same position. The symbols represent the position of the off-design points sideline

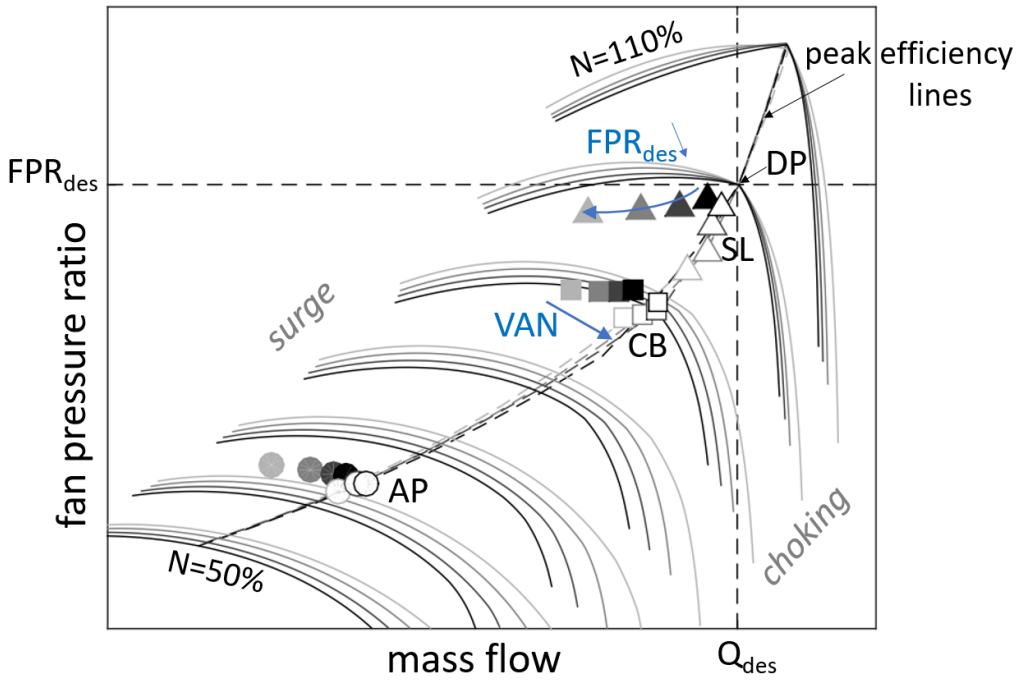

Figure 3: **Fan aerodynamic performance maps rescaled relative to the design point, and positions of the off-design operating points SL/CB/AP without VAN (colour-filled points) and with VAN (white points)**

(triangle), cutback (square) and approach (circle) within the fan map. The colour-filled symbols are for the case without VAN, and the white symbols are for the VAN case. As explained before, with VAN, the nozzle area opening is adjusted automatically to deliver the best aerodynamic efficiency, which is visible in the figure: all operating points are located along the lines of peak

efficiency (pictured as dashed lines), irrespective of the design FPR. In the case without VAN, the operating points are all located to the left from the peak-efficiency lines. As the design FPR decreases (colour code from dark to light grey), each of the three operating points moves further away from the peak-efficiency line and gets closer to the fan surge domain. As a result, the meanline methodology adopted in the present study captures properly the impact of the VAN on the location of the off-design operating points within the aerodynamic performance map. Also, the larger benefit of the VAN for low-presssure fans is predicted as expected.

AERODYNAMIC EVALUATION

In this section we examine in more details the change in aerodynamic conditions induced by a VAN implementation. The left part of Fig.4 shows the variations of nozzle area required to maximize the fan isentropic efficiency depending on the design value of the fan pressure ratio. The sideline, cutback, and approach points are depicted in red, magenta, and blue, respectively. In the middle and in the right part of Fig.4 respectively, the gains in surge margin and efficiency are shown with respect to the case without VAN. For the high-pressure fan (FPR=1.6) the gain

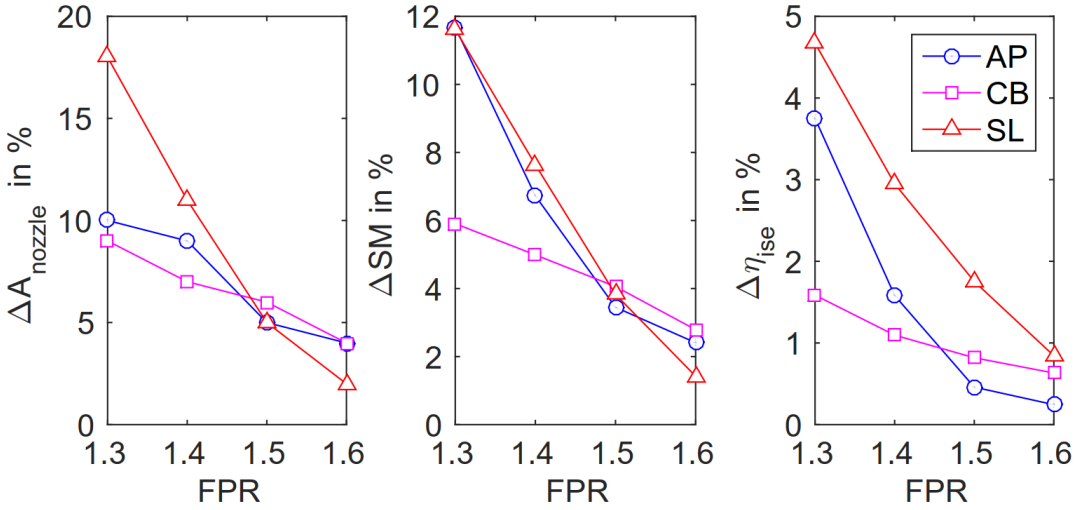

Figure 4: **Relative variations of nozzle area (left) and associated gains in surge margin (middle) and aerodynamic efficiency (right)**

in surge margin is less than 3% and less than 1% in efficiency, so the benefit is too small to justify a VAN implementation. As the design FPR decreases, both surge margin and efficiency are continuously improved, especially at take-off sideline and landing approach points, where a gain of 12% surge margin and 4% efficiency can be obtained with an area opening of 18% for the low-pressure fan with FPR=1.3. In practice, the surge margin without VAN is so low at approach or sideline conditions that safe operation of a low-pressure fan requires the implementation of a variable-geometry system.

The next Figure 5 shows the variations of Mach numbers, rotor incidence and rotor loss coefficients, in the nominal case without VAN. In the left part of Fig.5, the solid lines refer to the rotor tip relative Mach number, M_{tr}, and the dashed lines refer to the jet exhaust Mach number, M_j. We observe that all Mach number quantities decrease when decreasing the design fan pressure ratio. This is one the main drivers toward high propulsive efficiency and low noise typical of large engines powered by a low-pressure fan. Note that for FPR=1.3, the rotor operates under subsonic conditions during the whole take-off phase (sideline and cutback). In

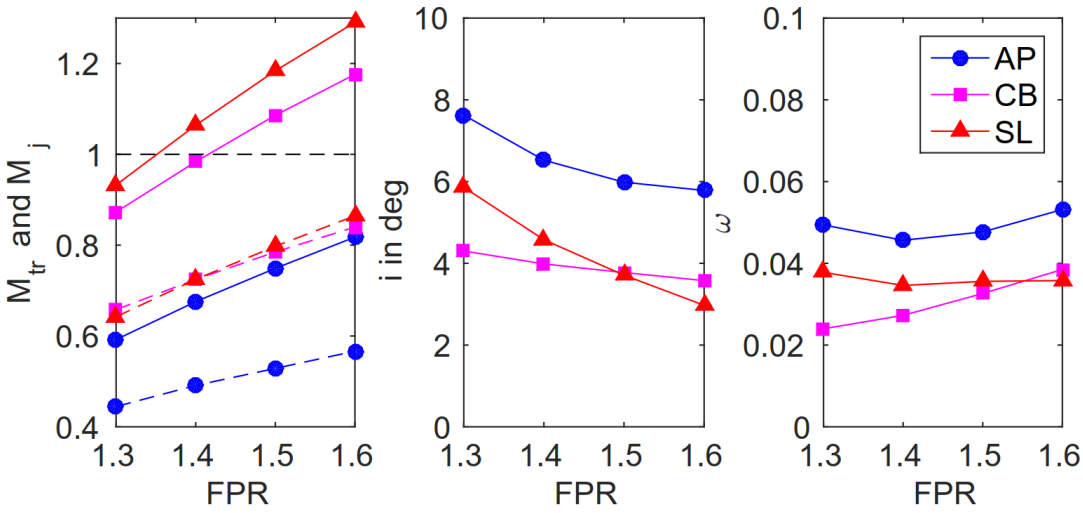

Figure 5: **Variations for each fan configuration without VAN of jet exhaust and tip relative Mach numbers (left), rotor incidence (middle) and rotor loss coefficient (right)**

the middle of the figure, the rotor incidence at the meanline radius gives indications about the severity of the off-design conditions where the fan operates. In general, the incidence increases with decreasing design FPR, the rise being particularly pronounced for the sideline point. At approach condition, the incidence is high (i>6 deg) even for the high-pressure fans, which is associated with poor performance and high aerodynamic loss, as can be seen in the right part of the figure.

The last figure 6 of this section shows the difference between the cases with and without VAN. The impact of the VAN is relatively small on the Mach numbers: as the design FPR diminishes, the rotor tip relative Mach number is increased by a few percents due to the nozzle opening and the increased throughflow through the fan, the jet exhaust Mach number is reduced by up to 6% mostly due to a reduction of the pressure ratio at which the fan operates, this will affect jet noise favourably. The VAN technology allows operation at much lower incidence levels, and accordingly lower loss, with reductions by up to 4.5 deg and 75%, respectively. The large sensitivity of loss to incidence is explained by the physical assumptions underlying the model chosen in this study (Freeman and Cumspty, 1992): this approach assumes thin and weakly cambered rotor blades with a sharp leading edge, which are typical of high-speed fans. Such blade profiles are well suited for supersonic inflow but tend to trigger early flow separation - thus higher losses and larger mean wakes - as soon as they operate under incidence in subsonic conditions. For the low pressure ratio fans, having blades with a rounded leading edge designed for subsonic inflow, this model probably overestimates the loss dependency on incidence. We will see in the next section that there is an acoustic benefit related to the reduction in incidence and loss.

ACOUSTIC EVALUATION

The noise results are presented in this section in a similar manner to that of the previous section. The variations of noise component levels are shown depending on the design fan pressure ratio for each of the three acoustic certification points SL, CB, and AP. We consider three different components for the acoustic evaluation of the engine. The first component is the broadband jet mixing noise; the other two components are related to the fan. The fan tonal noise is

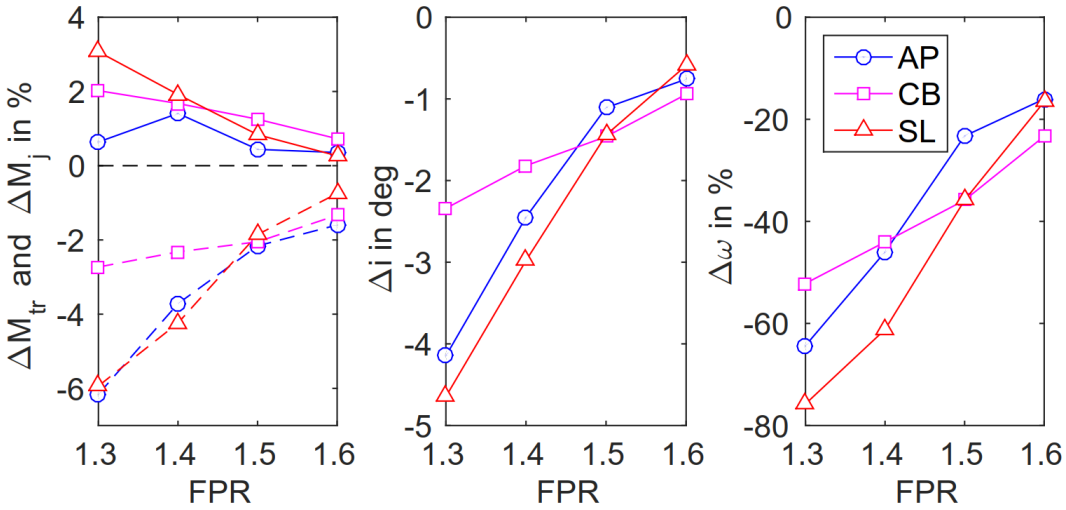

Figure 6: **Relative variations of jet exhaust and tip relative Mach numbers (left), rotor incidence (middle) and rotor loss coefficient (right), comparison with VAN vs. without VAN**

asssumed to be dominated by the rotor-stator wake interaction contribution and by the the rotor-self noise or buzz-saw noise contribution, prevalent only at supersonic tip speeds. The potential field interactions can be neglected owing to the large blade and vane counts, and the rotor is assumed to operate in a clean inflow, so its interaction with an incoming flow distortion is not modelled. Finally, the third component is the fan broadband noise, which is dominated by the interaction of the turbulent flow downstream of the rotor with the stator vanes. The trailing edge noise sources are considered of secondary order and are not modelled.

As can be seen in Fig.7, lowering the design FPR has the well-known effect of reducing jet noise drastically at all operating points, which is attributable to the lower jet Mach numbers observed in Fig.5. In general, both fan tonal and broadband noise are the results of competing mechanisms: the reduction of Mach numbers within the stage is acoustically beneficial but is partly offset by an increase in incidence-related loss (see Fig.5) and a more compact stage where the axial gap between rotor and stator is reduced compared to the dimensions of the fan blades (see Fig.2). Other mechanisms related to the coherent or non-coherent nature of fan noise sources explain the different behaviour of fan tonal and broadband noise, respectively. For fan tonal noise the reduction is substantial when the design allows for subsonic relative tip speed of the rotor, which is the case at the take-off points SL and CB for FPR$<$1.4. At approach conditions however, the analytical model (solid blue line) predicts a large increase of this source, which the NASA correlations (dashed blue lines) do not. This different behaviour is attributed to the effect of hub-to-tip wake tilting described by Envia (1999) - a source of strong destructive interferences for coherent sound sources, not captured by the NASA correlations - which becomes more pronounced as the intra-stage axial gap and the intra-stage swirl increase, as is the case for the high-speed designs. For fan broadband noise, the overall benefit from low-pressure fans is much less marked than the reduction of fan supersonic tonal noise, because unlike the rotor-locked potential field, the sound field excited by broadband sources remains cut-on even at lower speeds. Note that the empirical and analytical methods (resp. dashed and solid lines in the middle and right parts of the figure) differ in absolute level predictions but agree relatively well in terms of trends.

In this paper, only the changes in overall sound power are examined quantitatively but the

spectral distribution of sound power also affects the effectively perceived noise levels on the ground after its propagation through the atmosphere. In that respect, the acoustic benefit from low-speed fans is expected to be further tempered mainly due to two factors: the liner damping effectiveness and the atmospheric absorption. As shown in Table 2, the blade passing frequency f_{BPF} drops by a factor 3 from the high-speed fan at FPR=1.6 (f_{BPF}=2kHz) to the low-speed fan at FPR=1.3 (f_{BPF}=0.7kHz); the spectral distribution of the fan tonal and broadband noise components scales approximately with the blade passing frequency. This very substantial shift towards low frequencies is likely to impact negatively the performance of conventional single-degree-of-freedom liners, because this would imply that the liner cell depth has to be enlarged by a factor 3 to be optimally designed for the target frequency band, but this is unfeasible due to integration limitations in the nacelle (Sugimoto, 2010). Moreover, low-frequency sound is less well absorbed by the atmosphere.

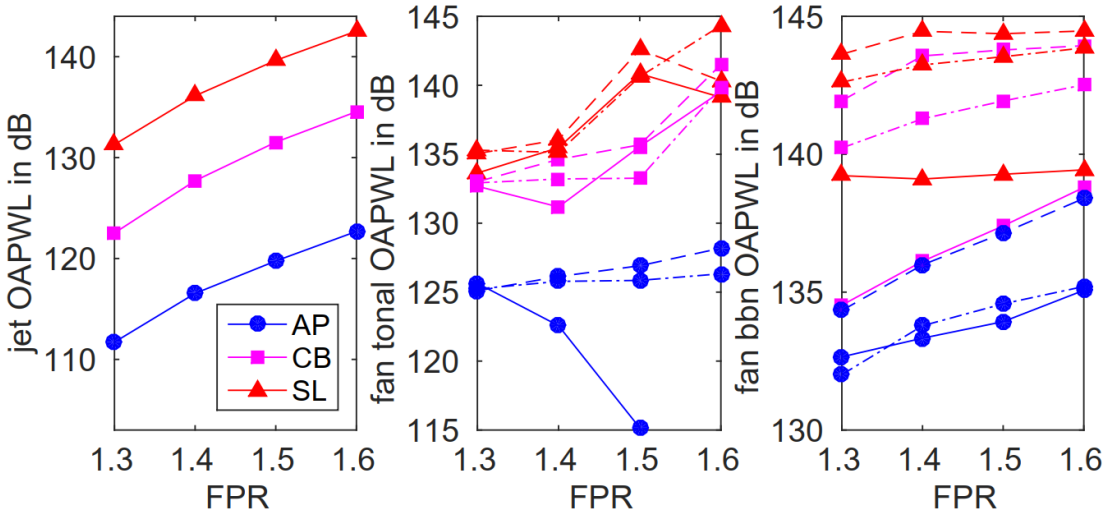

Figure 7: **Noise emissions of the fan stages without VAN (jet noise: left, fan tonal noise: middle, fan broadband noise: right)**

The acoustic benefit of the VAN is illustrated in Fig.8. The reduction of jet noise is in the order of a few decibels, up to 3 dB for the low-pressure fan with FPR=1.3. This reduction is directly attributable to the slight decrease in jet exhaust Mach number observed in Fig.5. This result is also in line with predictions by Michel (2011). In the middle of Fig.8, the evolution of fan tonal noise as predicted by the analytical approach (Moreau, 2017, solid lines) and by the two NASA correlations (Kontos, 1996, and Krejsa, 2014, dashed lines) shows a similar reduction by a few decibels, however the benefit predicted by the analytical method is significantly smaller than that predicted by the NASA correlations. Actually, for the approach conditions (circle symbols), the case with VAN is even noisier by around 2 dB than without VAN according to that method. This result is also in line with an experimental study by NASA (Woodward, 2004, 2006). The reduction of the flow swirl behind the rotor, induced by the aerodynamic unloading effect of the VAN, may lead to less radial dephasing of the rotor wakes when impinging onto the stator vanes, and may explain why tonal levels are higher with a VAN - this is again the wake tilting effect already mentionned and detailed by Envia (1999); this effect becomes dominant at approach as the rotor speed is subsonic and buzz-saw noise is non-existent.

Finally, the variations of fan broadband noise are given in the right part of the figure. For this source, the benefit from the VAN is clear and it steadily increases with decreasing design

FPR. Both the analytical method and the NASA correlations agree qualitatively about that trend, but the former predicts a much larger benefit, up to 12 dB at sideline for the low-pressure fan with FPR=1.3. The correlation by Kontos only predicts a benefit of 1.5 dB, whereas Krejsa's correlation provides around 3.5 dB. These differences between the methods are mostly due to the sensitivity of the acoustic models to the aerodynamic unloading effect of the VAN. As seen in Eq.(2), the larger value for the exponent n in Krejsa's model explains why unloading the fan (decreasing ΔT_t in the formula) yields a larger noise reduction than in Kontos' model. Concerning the analytical method, noise is directly related to the loss coefficient ω in Eq.(1), because this quantity represents the rotor wake size, which is the physical driver for the rotor-stator interaction mechanism. As ω is reduced by up to 75% (see Fig.6), the sound power scaling law with ω^2 explains the reduction in the order of 12 dB. Such prediction largely overestimates however the broadband noise reduction observed experimentally during the NASA experiments (Woodward, 2004, 2006). As mentionned during the discussion of the aerodynamic results, the loss model by Freeman and Cumpsty (1992) assumes sharp-nose blade profiles which generate more loss at off-design subsonic conditions than profiles with a rounded leading edge. Hence, the acoustic benefit from a reduction in incidence may be overestimated by a few decibels in the present analytical model, especially in the case of low pressure ratio fans.

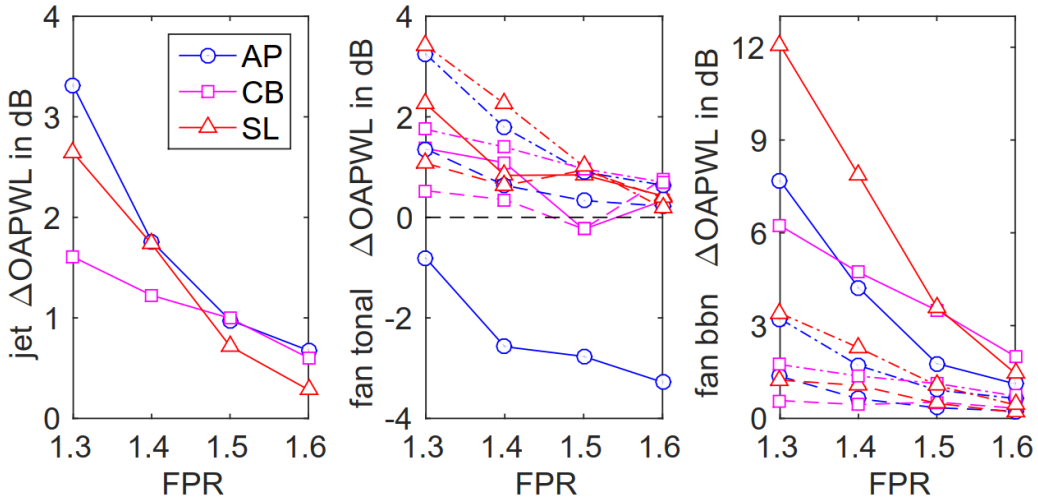

Figure 8: **Noise reductions achieved with VAN as predicted by several methods (fan noise: solid/dashed lines are for analytical/empirical methods, resp.)**

CONCLUSIONS

With the reduction of the design FPR, the acoustic certification points move closer to the surge limit of the fan. This is accompanied by an increase in incidence, higher loss, and larger wakes, which produce more broadband noise when impinging onto the stator vanes. This effect partly offsets the acoustic benefit obtained from the low Mach number levels that can be realised in low-pressure fans. In all, the decrease in fan broadband noise for these engines is not as high as the one achieved in terms of jet noise or even fan tonal noise, which also implies that fan broadband noise dominates in UHBR engines. In addition to that, large low-speed engines with less rotor blades generate sound fields in a much lower frequency range (a factor 3 is estimated between designs with FPR=1.3 and FPR=1.6). This strong shift toward low frequencies further reduces the acoustic potential of these large engines, as both liners and atmospheric absorption are less effective at reducing low-frequency sound.

With the implementation of a variable-area nozzle, whose opening has to reach 10% to 20%, the operating points are moved back onto the line of peak efficiency inside the fan map, with a substantial improvement in surge margin by 10% or more and an aerodynamic efficiency improvement by up to 5%. The mechanism is basically to increase the throughflow through the stage and to unload the fan blades, so the Mach numbers are slightly increased but the incidence and losses are very substantially reduced. These aerodynamic results provided by the present meanline approach agree well with past theororetical studies.

The variable-area nozzle also has a large impact on noise. Jet noise is found to be reduced by 2-3 dB, which is in line with a previous estimation. A novel aspect addressed in the paper is also the acoustic benefit to be expected in terms of fan noise. Fan tonal noise is hardly impacted at high speed, but slightly increased at low speed which is not a risk as fan tones do not dominate there. More importantly, fan broadband noise is very significantly decreased. All prediction methods agree qualitatively about these trends, and they are also in line with previous experiments conducted by NASA; the main difference between the methods lies in the magnitude of the expected reduction: the analytical method based on the wake size of sharp-nose blades predicts a much larger broadband noise reduction (around 10 dB) than the empirical correlations based on global thermodynamic parameters (around 2-3 dB). It should be noted here that the presence of a VAN is not expected to affect much the liner damping or the perceived noise after propagation through the atmosphere, as the change in rotation frequencies due to a VAN is fairly small.

In summary, the variable-area nozzle is aerodynamically beneficial in extending the surge margin and improving the fan isentropic efficiency and the global propulsive efficiency of the engine. However, its implementation is mechanically complex and associated with a weight penalty. Acoustically, it must be considered to reduce primarily jet and fan broadband noise at the source, but not necessarily fan tonal noise. At low pressure ratios around FPR=1.3, a variable-geometry system seems mandatory to enable off-design operation, but in that case the required VAN opening by 20% is large.

Future work will consider the acoustic impact of a variable-pitch fan system, which represents an alternative solution to the variable-area nozzle, and may even be the technology of choice for engine fans with a very low design pressure ratio below 1.3. Also, the very substantial reduction in fan broadband noise observed with the loss model assuming sharp-nose blades may be tempered if the model assumes well-designed rounded leading edges more representative of low-speed fan blades. Hence, the impact of the correlation chosen between incidence and loss is also a question worth investigating.

ACKNOWLEDGEMENTS

The author thanks the DLR-funded research projects KonTeKst and SIAM for supporting financially this study. The author is also grateful to Prof. Ulf Michel, for his helpful remarks on the paper and on the topic of variable-area nozzle technology.

REFERENCES

Cumpsty, N., (2009). *Preparing for the future: reducing gas turbine environmental impact*. ASME Turbo Expo 2009, Orlando, Florida, paper GT2009-60367.

Envia, E. and Nallasamy, M., (1999). *Design selection and analysis of a swept and leaned stator concept*. Journal of Sound and Vibration, Vol. 228, pp.793-836, 1999.

Freeman, C. and Cumpsty, N., (1992). *Method for the prediction of supersonic compressor blade performance*. Journal of Propulsion, Vol.8, pp.199-208, 1992.

Giannakakis, P., (2013). *Design space exploration and performance modelling of advances*

turbofan and open-rotor engines. PhD Thesis, Cranfield University, UK.

Guynn, M., et al., (2011). *Refined exploration of turbofan design options for an advanced single-aisle transport*. NASA Technical Memorandum TM-2011-216883.

Kavvalos, M. and Zhao, X. and Schnell, R. and Aslanidou, I. and Kalfas, A. and Kyprianidis, K., (2019). *A modelling approach of variable geometry for low-pressure-ratio fans*, ISABE Conference, paper ISABE-2019-24382.

Kontos, K. and Janardan, B. and Gliebe, P., (1996). *Improved NASA-ANOPP noise prediction computer code for advanced subsonic propulsion systems, Vol.1*, NASA Contractor Report 195480.

Krejsa, E. and Stone, J., (2014). *Enhanced fan noise modelling for turbofan engines*, NASA Contractor Report 2014-218421.

Kyritsis, V, (2006). *Thermodynamic preliminary design of civil turbofans and variable geometry implementation*, PhD thesis, Cranfield University, UK.

Merkl, E., et al., (2018). *Engine Module Validators for UHBR aero-engines*. ENOVAL final report, EU Horizon 2020 project FP7-604999.

Michel, U., (2011). *The benefits of variable-area fan nozzle on turbofan engines*. 49th AIAA Aerospace Sciences Meeting including the New Horizons Forum and Aerospace Exposition, Orlando, Florida, paper AIAA-2011-0226.

Moreau, A., (2017). *A unified analytical approach for the acoustic conceptual design of fans of modern aero-engines*. PHD thesis, Technical University of Berlin, 2017.

Moreau, A. and Guérin, S., (2020). *Experimental validation of an analytical prediction model for fan buzz-saw noise*. ASME Turbo Expo 2020, planned venue London, organized as Virtual Event, paper GT2020-14279.

Sain, C. and Hoeschler, K. and Mischke, M., (2015). *Concept study of variable-area fan nozzle for utlra-high bypass ratio*. ISABE Conference, paper ISABE-2015-22165.

Stone, J. and Groesbeck, D., and Zola, C., (1983). *Conventional profile coaxial jet noise prediction*. AIAA Journal, Vol.21, pp.336-342.

Sugimoto, R. and Astley, J. and Murray, P. (2010). *Low-frequency liners for turbofan engines*. Proceedings of the 20th International Congress on Acoustics, Sydney, 2010.

Woodward, R. and Hughes, C., (2004). *Noise benefits of increased fan bypass nozzle area*. NASA Technical Memorandum TM-2004-213396 (also published as conference paper AIAA-2005-1201).

Woodward, R. and Hughes, C. and Podboy, G., (2006). *Fan noise reduction with increased bypass nozzle area*. Journal of Aircraft, Vol. 43, pp.1719-1725.